

X-321-67-97

NASA-TM-X-55743

FINITE ELEMENT MODELING OF A CANTILEVER BEAM

BY

JERRY F. KUZANEK

N 67-22881

FACILITY FORM 602

(ACCESSION NUMBER)

(PAGES)

(NASA CR OR TMX OR RD NUMBER)

(THRU)

(CODE)

(CATEGORY)

MARCH 1967

NASA

GODDARD SPACE FLIGHT CENTER
GREENBELT, MARYLAND

**FINITE ELEMENT MODELING
OF A
CANTILEVER BEAM**

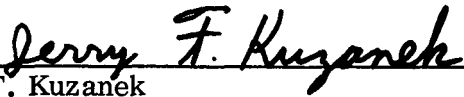
**By
Jerry F. Kuzanek
Test and Evaluation Division
Systems Reliability Directorate**

March 1967

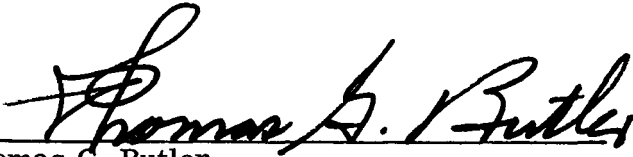
**Goddard Space Flight Center
Greenbelt, Maryland**

FINITE ELEMENT MODELING
OF A
CANTILEVER BEAM

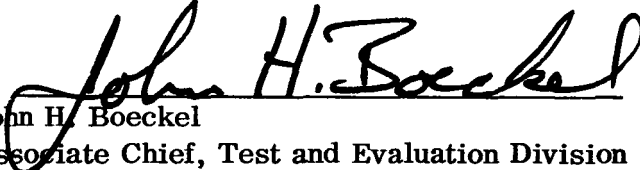
Prepared by:


Jerry F. Kuzanek
Structural Analysis Computer Group

Reviewed by:


Thomas G. Butler
Head, Structural Analysis Computer Group

Approved by:


John H. Boeckel
Associate Chief, Test and Evaluation Division

Project Status

The present report is one of a series of finite element modeling studies which is to be used as a basis for a handbook of modeling techniques.

Authorization

Test and Evaluation Division charge No. 321-124-08-05-14

CONTENTS

	Page
ABSTRACT	vii
1. INTRODUCTION	1
2. THEORETICAL SOLUTIONS	2
3. FINITE ELEMENT MODELS	5
Three Digit Bending Model	5
Two Digit Bending Model	6
Diagonal Model	9
EXAMPLES	16
1" \times 1" \times 25" Aluminum Cantilever Beam	16
10" \times 5" \times 25" Aluminum Cantilever Beam	22
4. CONCLUSIONS.	26
REFERENCES.	26

ILLUSTRATIONS

Figure		Page
1	Three Digit Bending Model (n Partitions)	6
2	Two Digit Bending Model (n Partitions)	7
3	Slice of Beam	8
4	Diagonal Model (n Partitions)	10
5	Beam and Diagonal Model Segment	12
6	Shear Deformation of a Diagonal Model Segment	13
7	Shear Forces Acting at the Grid Points of a Diagonal Model Segment	15

TABLES

		Page
I	Input to the Structural Analysis Computer Program for Finite Element Models with 25 Partitions of a 1" × 1" × 25" Aluminum Cantilever Beam	17
II	Frequencies of a 1" × 1" × 25" Aluminum Cantilever Beam According to the Three Theories and Three Models with 25 Partitions	18
III	Frequencies of a 1" × 1" × 25" Aluminum Cantilever Beam According to the Timoshenko Theory and the Diagonal Model with 50 Partitions	19
IV	Fifth Mode Shape of a 1" × 1" × 25" Aluminum Cantilever Beam	20
V	Tenth Mode Shape of a 1" × 1" × 25" Aluminum Cantilever Beam	21
VI	Frequencies of a 10" × 5" × 25" Aluminum Cantilever Beam	24
VII	Fourth, Fifth, and Eleventh Mode Shapes of a 10" × 5" × 25" Aluminum Cantilever Beam	25

FINITE ELEMENT MODELING
OF A
CANTILEVER BEAM

By

Jerry F. Kuzanek
Goddard Space Flight Center

ABSTRACT

Three finite element models of uniform beams were designed for digital computer analysis in an effort to approximate the first twenty-five transverse frequencies and mode shapes of a 1" \times 1" \times 25" aluminum cantilever beam. The first model accounted for only the bending properties in the beam; the second model accounted for rotatory inertia in the beam in addition to bending; and the third model accounted for shear flexibility in the beam in addition to bending and rotatory inertia. The results from the first model were compared with the results according to the Bernoulli-Euler theory of the transverse vibrations of uniform beams; those from the second model with those according to the Rayleigh theory; and those from the third model with those according to the Timoshenko theory. In general, the agreement between model and theory was excellent.

In order to ascertain the applicability of the third model to thicker beams, in which shear flexibility becomes increasingly more important, an aluminum cantilever beam 10" thick, 5" deep, and 25" long was considered. Once again the agreement between the finite element model and the applicable Timoshenko theory was excellent.

FINITE ELEMENT MODELING OF A CANTILEVER BEAM

by

Jerry F. Kuzanek

1. INTRODUCTION

A finite element model of an elastic structure consists of a scheme for representing the mass properties at a finite number of points and the elastic properties among these points. Formally, the representations of elastic properties are known as structural elements of the model and their points of connection are known as grid points. The mass and rotatory inertia of the structure are distributed at the grid points of the model. Hence the uniform distribution of mass of the structure is approximated by the lumped distribution of mass of the model. The static and dynamic equations for the model are then solved through the use of a structural analysis computer program in order to determine the static and dynamic characteristics of the model.

For the results presented in this paper, the Martin Company's SB038 structural analysis "force method" computer program was used to obtain only the dynamic characteristics of three finite element models of a cantilever beam. In order to determine dynamic characteristics, this structural analysis program requires the following six categories of input:

- (a) Coordinates of grid points.
- (b) Directions of equations of equilibrium at each grid point.
- (c) Dynamic degrees of freedom at each grid point.
- (d) Mass and moments of inertia at each grid point.
- (e) Types of structural elements at or between grid points.
- (f) Compliances of these structural elements.

The value of a finite element model is realized by its being able to obtain approximations to both the static and dynamic characteristics of a complex structure, of which the exact characteristics are unobtainable due to the impossibility of solving the equations describing the elastic behavior of that structure. Of course, it is quite possible that improper modeling may result in the

characteristics of the model being entirely different from the true characteristics of the structure, and the analyst, having no reference with which to compare these characteristics of the model, would be unaware of these differences. However, if the analyst were to model simple structures, for which theoretical results are available, he would be able to assess the applicability of his models to these simple structures through a comparison of the characteristics of his models to the characteristics of the simple structures. The methods used to obtain the best models could then be applied to more complicated structures.

The purpose of this report is to establish methods for the finite element modeling of a particular simple structure, namely a uniform, isotropic, cantilever beam. It should be emphasized that the first, second, and third finite element models discussed in this paper attempt to account for only those properties of a cantilever beam which are accounted for by the Bernoulli-Euler, Rayleigh, and Timoshenko theories respectively. Furthermore, these three finite element models may be used to model uniform beams with end conditions different from clamped-free merely by modifying the reaction elements at the ends of these models.

2. THEORETICAL SOLUTIONS

The following frequency and modal equations for the transverse vibrations of a uniform cantilever beam according to the Timoshenko theory were obtained from reference (1). The frequency and modal equations according to the Rayleigh and Bernoulli-Euler theories are special cases of these.

The following notation is used:

- y = Coordinate along length of beam
- z = Coordinate of lateral displacement
- L = Length of beam
- A = Cross sectional area
- ρ = Density
- E = Young's modulus
- G = Shear modulus
- I = Area moment of inertia of cross section
about bending axis

$k' =$ Timoshenko's shear coefficient
 $\omega =$ Frequency of vibration in radians per second
 $\sigma = A\rho =$ Mass per unit length of beam
 $B = EI =$ Bending stiffness
 $C = k' AG =$ Shear stiffness
 $s = \sqrt{I/A} =$ Radius of gyration of beam cross section.
 $\xi = y/L =$ Lengthwise position variable
 $\eta = z/L =$ Lateral displacement variable
 $\phi = \omega L^2 \sqrt{\sigma/B} =$ Frequency parameter
 $\alpha = B/CL^2 =$ Parameter proportional to shear flexibility
 $\beta = s^2/L^2 =$ Parameter proportional to rotatory inertia.
 $p^2 = \frac{1}{2} \left\{ \phi^2 (\alpha + \beta) + \sqrt{\phi^4 (\alpha - \beta)^2 + 4\phi^2} \right\}$
 $q^2 = \frac{1}{2} \left\{ -\phi^2 (\alpha + \beta) + \sqrt{\phi^4 (\alpha - \beta)^2 + 4\phi^2} \right\}$

There are two frequency and two modal equations for the transverse vibrations of a cantilever beam according to the Timoshenko theory depending upon whether q^2 is positive or negative. If q^2 is positive then the frequency equation is

$$2 + \{2 + \phi^2 (\alpha - \beta)^2\} \cos p \cosh q - \phi^2 (\alpha + \beta) \frac{\sin p}{p} \frac{\sinh q}{q} = 0, \quad (2.1)$$

and the corresponding modal equation is

$$\begin{aligned}
K\eta = & \left(\frac{\sin p}{p} - \frac{\sinh q}{q} \right) \{ p (q^2 + \phi^2 \alpha) \sin p \xi - q (p^2 - \phi^2 \alpha) \sinh q \xi \} \\
& + \{ (q^2 + \phi^2 \alpha) \cos p + (p^2 - \phi^2 \alpha) \cosh q \} (\cos p \xi - \cosh q \xi),
\end{aligned} \quad (2.2)$$

in which ϕ is a solution of (2.1), and K is an arbitrary constant.

If q^2 is negative, we put $q^2 = -r^2$, so that the frequency equation becomes

$$2 + \{2 + \phi^2 (\alpha - \beta)^2\} \cos p \cos r - \phi^2 (\alpha + \beta) \frac{\sin p}{p} \frac{\sin r}{r} = 0, \quad (2.3)$$

and its corresponding modal equation becomes

$$K\eta = \left(\frac{\sin p}{p} - \frac{\sin r}{r} \right) \{ p(r^2 - \phi^2 \alpha) \sin p\xi - r(p^2 - \phi^2 \alpha) \sin r\xi \} \quad (2.4)$$

$$+ \{ (r^2 - \phi^2 \alpha) \cos p - (p^2 - \phi^2 \alpha) \cos r \} (\cos p\xi - \cos r\xi).$$

If bending and rotatory inertia are to be considered, but shear flexibility is to be regarded as infinite, then we obtain the frequency and modal equations according to the Rayleigh theory by putting $\alpha = 0$ in (2.1), (2.2) and in the expressions defining the quantities p^2 and q^2 . The frequency equation becomes

$$2 + (2 + \phi^2 \beta^2) \cos p \cosh q - \phi^2 \beta \frac{\sin p}{p} \frac{\sinh q}{q} = 0, \quad (2.5)$$

and the corresponding modal equation becomes

$$K\eta = (q \sin p - p \sinh q) (q \sin p\xi - p \sinh q\xi) \quad (2.6)$$

$$+ (q^2 \cos p + p^2 \cosh q) (\cos p\xi - \cosh q\xi).$$

It can be shown that when shear flexibility is considered to be infinite, q^2 is never negative, so that we only have one frequency and one modal equation in this case.

If only bending is to be considered, then the frequency and modal equations according to the Bernoulli-Euler theory are obtained by putting $\alpha = \beta = 0$ in (2.1), (2.2), and in the expressions defining the quantities p^2 and q^2 . It follows that $p^2 = q^2 = \phi$. The frequency equation becomes

$$1 + \cos \sqrt{\phi} - \cosh \sqrt{\phi} = 0, \quad (2.7)$$

and the modal equation becomes

$$K\eta = (\sin \sqrt{\phi} - \sinh \sqrt{\phi}) (\sin \xi \sqrt{\phi} - \sinh \xi \sqrt{\phi}) \quad (2.8)$$

$$+ (\cos \sqrt{\phi} + \cosh \sqrt{\phi}) (\cos \xi \sqrt{\phi} - \cosh \xi \sqrt{\phi}).$$

In order to obtain the solutions to equations (2.1) - (2.8), the author wrote a Fortran IV computer program for the IBM 7094 using double precision arithmetic. Incorporated in this program was the Share Library subroutine AI ROOT, which was modified from single to double precision.

3. FINITE ELEMENT MODELS

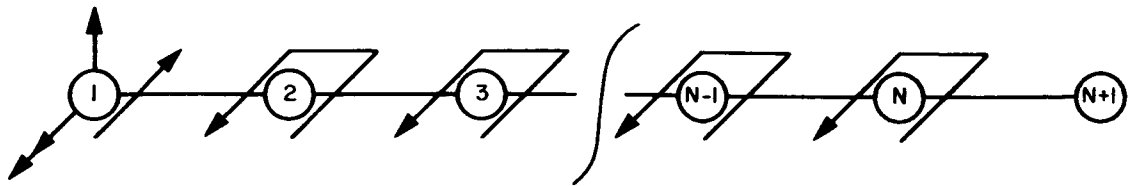
Three Digit Bending Model


The first model (Figure 1) is named a three digit bending model after the name of its dominant finite element. The three digit bending element is characterized by two linked linear elements with balanced moments at the joint. The grid points of this model are evenly spaced along a straight line with the first grid point at the origin of a Cartesian coordinate system. Transverse equations of equilibrium at each grid point and one moment equation of equilibrium at the first grid point are needed for equilibrium of the model. Moment equations of equilibrium at the other grid points are not needed because the three digit bending element establishes moment equilibrium internally. Dynamic degrees of freedom in the transverse direction are needed at all grid points except the first. The mass of the beam is uniformly distributed at the grid points of this model. Since no grid point has rotational degrees of freedom, no grid point can have moments of inertia assigned to it. Therefore, this model attempts to account for only the bending properties of uniform beams. Hence, its dynamic characteristics will be compared with those obtained from the Bernoulli-Euler beam theory.

At the first grid point, infinitely stiff axial and moment reaction elements are required to simulate the clamped end of the beam. A two digit bending element is placed between grid points one and two with bending at grid point one. The compliance of this element is given by

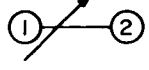
$$C = \ell / 3EI, \quad (3.1)$$

where ℓ is the distance between these grid points, E is Young's modulus and I is the area moment of inertia of a cross section of the beam about its bending axis. Three digit bending elements are placed among each consecutive triplet of grid points with balanced bending moments at the intermediate grid point. The compliance for these elements is given by equation (3.1) where ℓ is now the sum of the distances between the first pair and the second pair of points of a consecutive triplet of grid points. Since the grid points in this model are all evenly spaced along a straight line, the compliance of a three digit bending element for this model is twice that of a two digit bending element. Consecutive



 = AXIAL REACTION ELEMENT AT GRID POINT 1.

 = MOMENT REACTION ELEMENT AT GRID POINT 1.

 = TWO DIGIT BENDING ELEMENT BETWEEN GRID POINTS 1 AND 2 WITH BENDING AT GRID POINT 1.

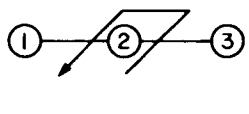
 = THREE DIGIT BENDING ELEMENT AMONG GRID POINTS 1, 2, AND 3 WITH BALANCED BENDING MOMENTS AT GRID POINT 2.

Figure 1—Three Digit Bending Model (n Partitions)

pairs of three digit bending elements are coupled to each other and their coupled compliance is given by

$$C = \ell / 12EI. \quad (3.2)$$

The two digit bending element between grid points 1 and 2 is coupled to the three digit bending element among grid points 1, 2, and 3, and the value of their coupled compliance is the same as that for the coupled compliance between consecutive three digit bending elements.

Two Digit Bending Model

The second model is named a two digit bending model (Figure 2), after the name of its dominant finite element. This model is essentially the same as the previous model with the exception that each three digit bending element is replaced by two two digit bending elements. There is a pair of two digit bending elements between each pair of consecutive grid points with the exception of the

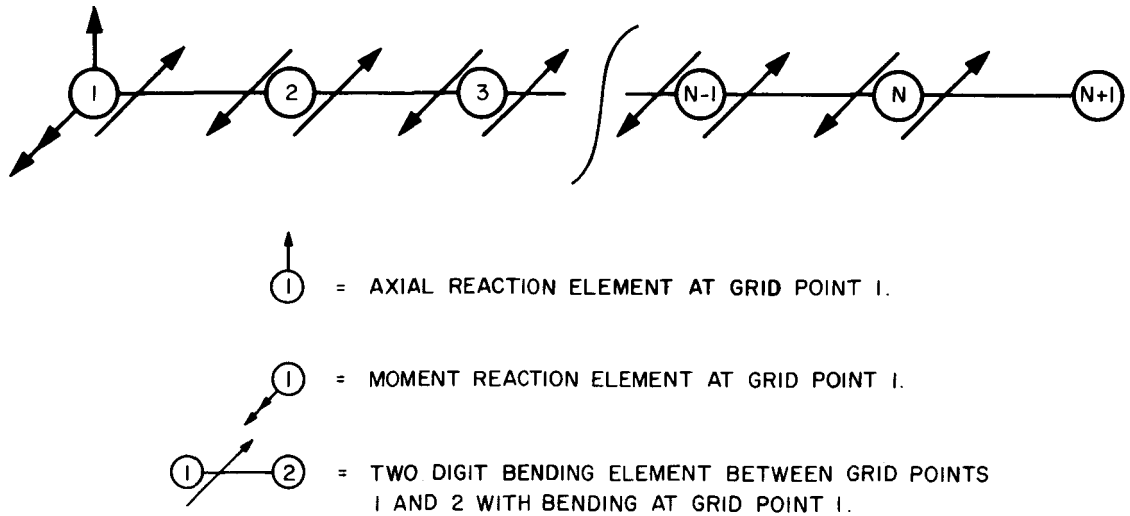


Figure 2—Two Digit Bending Model (n Partitions)

last pair. The compliance of each two digit bending element is given by equation (3.1) and the coupled compliance of each pair of two digit bending elements is

$$C = \ell / 6EI \quad (3.3)$$

where ℓ is its length. Transverse equations of equilibrium at all grid points and moment equations of equilibrium at all grid points except the last are needed for equilibrium of the model. Dynamic degrees of freedom in the transverse direction are assigned to all grid points except the first and rotational dynamic degrees of freedom are assigned to all grid points except the first and last. As in the previous model, the mass of the beam is uniformly distributed at the grid points of this model. Since this model has rotational degrees of freedom at all grid points except the first and last, moments of inertia can be assigned to these grid points in order to account for the rotatory inertia of the beam. This assignment has been made in the following way.

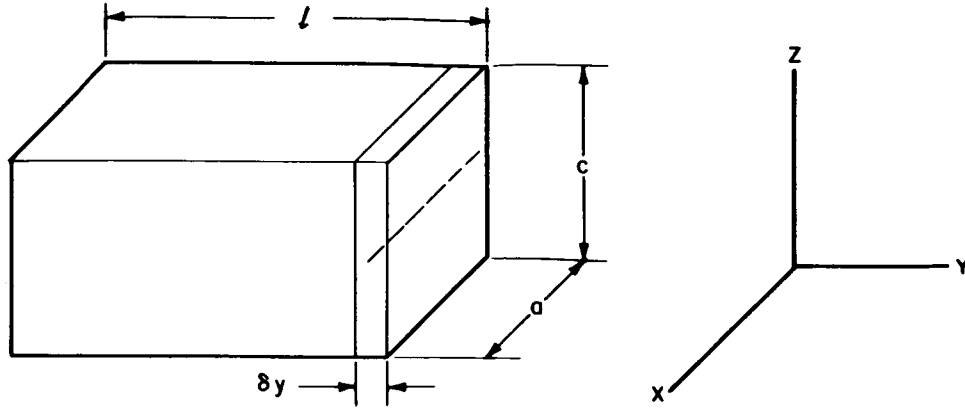


Figure 3-Slice of Beam

Suppose the distance between consecutive grid points is ℓ . Consider a thin slice of the beam of dimensions given in Figure 3. The moment of inertia of this slice about its neutral axis is

$$J_i = \frac{1}{V} \int_0^a \int_{-c/2}^{c/2} \int_{-\delta y_i/2}^{\delta y_i/2} m_i (y^2 + z^2) dy dz dx \quad (3.4)$$

$$= \frac{a c m_i \delta y_i}{12 V} (\delta y_i^2 + c^2),$$

where V is the volume of the slice and m_i is its mass. Since

$$V = \delta y_i a c, \quad (3.5)$$

we have

$$J_i = \frac{m_i}{12} (\delta y_i^2 + c^2). \quad (3.6)$$

Now if n of these slices comprise one beam segment of length ℓ then

$$n \delta y_i = \ell, \quad (3.7)$$

and

$$n m_i = m, \quad (3.8)$$

where m is the mass of this segment. Hence, the rotatory inertia of this segment is

$$\begin{aligned} J_b &= \lim_{\delta y_i \rightarrow 0} \sum_{i=1}^n J_i \\ &= \lim_{\delta y_i \rightarrow 0} \frac{n m_i}{12} (\delta y_i^2 + c^2) \\ &= \frac{m c^2}{12}. \end{aligned} \quad (3.9)$$

Since the grid points of this model are evenly spaced along a straight line, this is also the moment of inertia which is assigned to every grid point except the first and last. Therefore, this model attempts to account for both bending and rotatory inertia in uniform beams. Hence, its dynamic characteristics will be compared with those obtained from the Rayleigh theory.

Diagonal Model

The third model is named a diagonal model (Figure 4) primarily because it contains tension elements located in a diagonal direction. Their function is to simulate the additional consideration of shear flexibility in the beam.

The grid points of this model are evenly spaced along two parallel straight lines. Transverse and longitudinal equations of equilibrium are needed at each grid point for equilibrium of the model. Dynamic degrees of freedom in both the transverse and longitudinal directions are specified at all grid points except the first two. The mass of the beam on each side of the neutral plane is uniformly distributed at the corresponding grid points on each side of the neutral plane, so that the beam and the model have the same mass. If we require that the rotatory inertia of the model be equal to the rotatory inertia of the beam, then we can uniquely determine the distance h of the grid points from the neutral plane.

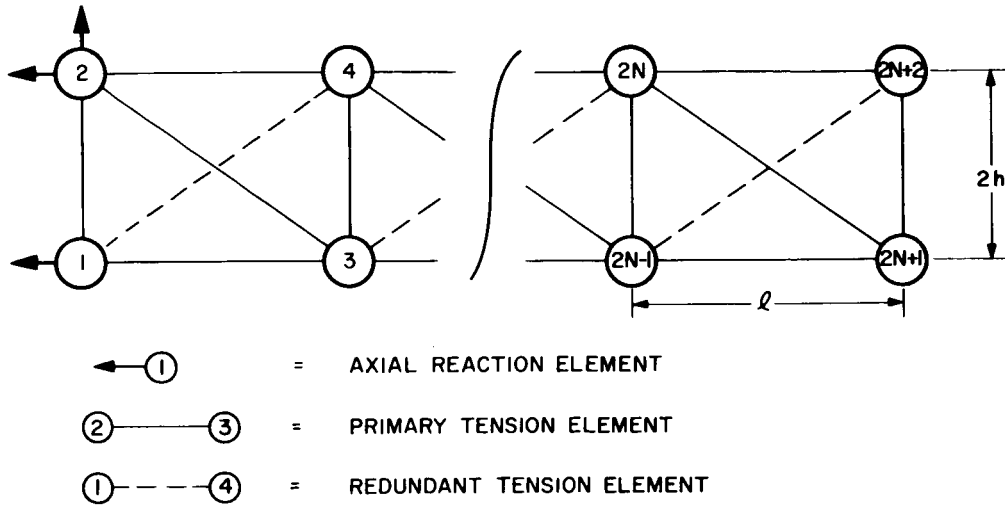


Figure 4-Diagonal Model (n Partitions)

The rotatory inertia of a beam segment of length l was given by

$$J_b = \frac{m c^2}{12} . \quad (3.9)$$

The moment of inertia of two masses $m/2$, each a distance h from the neutral axis is

$$J_m = 2 \left(\frac{m}{2} h^2 \right) = m h^2 . \quad (3.10)$$

Equating J_b and J_m yields

$$h = c / \sqrt{12} . \quad (3.11)$$

The area moment of inertia of a cross section of the beam is

$$I = \int_0^a \int_{-c/2}^{c/2} z^2 dz dx = \frac{a c^3}{12} , \quad (3.12)$$

and by putting $A = ac$, this becomes

$$I = \frac{A c^2}{12} . \quad (3.13)$$

Combining (3.11) with (3.13) yields

$$h = \sqrt{\frac{I}{A}} . \quad (3.14)$$

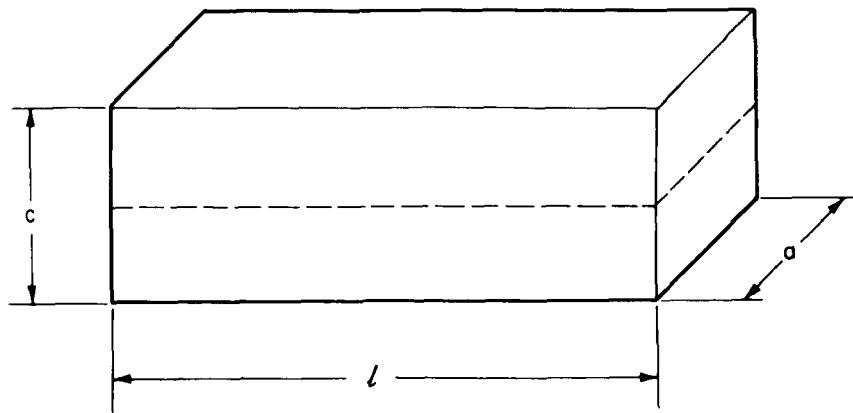
Infinitely stiff axial reaction elements in the longitudinal direction at grid points one and two and an infinitely stiff axial reaction element in the transverse direction at either grid point one or two are required to simulate the clamped end of the beam. The transverse tension elements are infinitely stiff so that Poisson coupling is not considered in this model, just as it is not considered in the Timoshenko theory of the transverse vibrations of uniform beams.

In order to determine the compliance of the longitudinal tension elements we divide the beam and the model into segments, as in Figure 5. It can be seen that the longitudinal tension elements will contribute solely to the effects of bending during the transverse vibrations of the beam. If a moment M is applied to the end of a beam segment and to the end of a model segment, then we shall require that a fiber of length ℓ in the beam, a distance h from the neutral plane, undergo the same deformation as a longitudinal tension element in the model, which is also a distance h from the neutral plane. From the theory of the bending of beams, the deformation of this fiber is

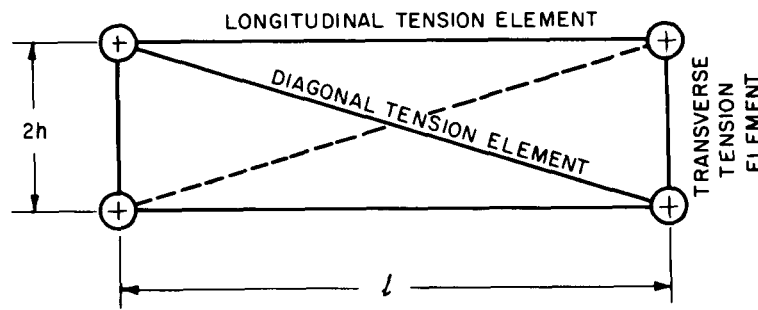
$$\delta_b = \frac{\ell h M}{EI} . \quad (3.15)$$

When this moment M is applied to a model segment, it is equivalent to applying equal and opposite forces of magnitude

$$F = \frac{M}{2 h} \quad (3.16)$$



a) BEAM SEGMENT



b) DIAGONAL MODEL SEGMENT

Figure 5—Beam and Diagonal Model Segment

to the two longitudinal tension elements, whose compliances are given by

$$C_{\ell} = \frac{\delta_m}{F} \cdot \quad (3.17)$$

Replacing δ_m by the value of δ_b in (3.15), using (3.16), and noting that $h = \sqrt{I/A}$ from (3.14), we have as the compliance of the longitudinal tension elements

$$C_{\ell} = \frac{2\ell}{EA} \cdot \quad (3.18)$$

In order to determine the compliance of the diagonal tension elements, notice is taken of the fact that due to the pin connection of the points, these elements will contribute solely to the effects of shear flexibility during the transverse vibration of the beam, as can be seen in Figure 6. By applying a given shear force to a cross section of a beam segment and an equivalent shear force at the grid points of a model segment, we require that the angle of shear γ at the neutral axis of the beam be the same as the angle of shear $\bar{\gamma}$ at the neutral axis of the model. We note that since the transverse tension elements cannot carry bending loads, the angle of shear $\bar{\gamma}$ in the model is the same at any distance, measured in a transverse direction, from the neutral axis, so that we may speak of "the angle of shear $\bar{\gamma}$ " without specifying its location with respect to the neutral axis.

The length of the diagonal tension element, before any deformation occurs, is

$$\ell_0 = (\ell^2 + 4h^2)^{1/2}, \quad (3.19)$$

where ℓ and h are as in figure 5. After a shear deformation, its length becomes

$$\ell_1 = \left((\delta + 2h)^2 + (\ell^2 - \delta^2) \right)^{1/2}, \quad (3.20)$$

according to figure 6. Putting $\bar{\gamma} = \delta/\ell$, this becomes

$$\ell_1 = (4\bar{\gamma}\ell h + 4h^2 + \ell^2)^{1/2}, \quad (3.21)$$

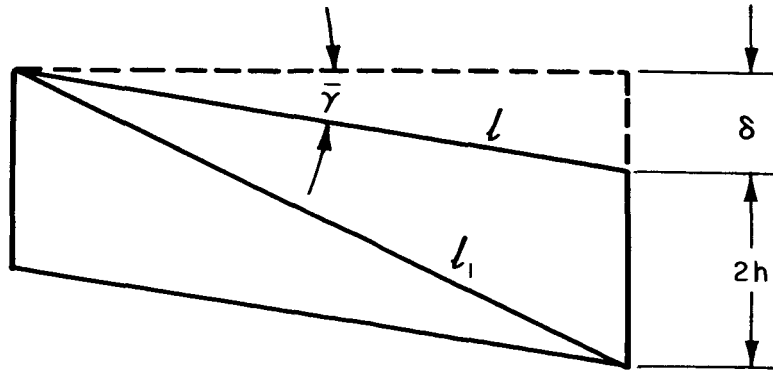


Figure 6—Shear Deformation of a Diagonal Model Segment

which may be expressed as,

$$\ell_1 = (4h^2 + \ell^2)^{1/2} \left(\frac{4\bar{\gamma} \ell h}{4h^2 + \ell^2} + 1 \right)^{1/2}. \quad (3.22)$$

Expanding the second term on the right hand side by the binomial theorem and disregarding terms of order greater than one in $\bar{\gamma}$, we have the approximation

$$\ell_1 \approx (4h^2 + \ell^2)^{1/2} \left(1 + \frac{2\bar{\gamma} \ell h}{4h^2 + \ell^2} \right). \quad (3.23)$$

Hence the extensional deformation of this diagonal tension element is

$$\delta_1 \approx \ell_1 - \ell_0 = \frac{2\bar{\gamma} \ell h}{(4h^2 + \ell^2)^{1/2}}. \quad (3.24)$$

Now suppose a shear force V is applied to both cross sections of a beam segment. An equivalent shear force in the model segment with one diagonal tension element removed (Figure 7) can be obtained by applying forces of magnitude $V/2$ to the four grid points of the model segment, in the same direction as the shear forces acting on the beam segment. In order to maintain rotational equilibrium of this segment, we must have forces of magnitude $V\ell/4h$, acting at the four grid points of this segment, in the direction of the longitudinal tension elements. The resultant tension T_1 in the diagonal tension element is

$$T_1 = \frac{V}{2h} (4h^2 + \ell^2)^{1/2}. \quad (3.25)$$

If we assume that both diagonal tension elements carry the same load, then the tension in each of them is

$$T = \frac{T_1}{2} = \frac{V}{4h} (4h^2 + \ell^2)^{1/2}. \quad (3.26)$$

If Q is the average shear stress on a cross section of the beam then

$$Q = \frac{V}{A}, \quad (3.27)$$

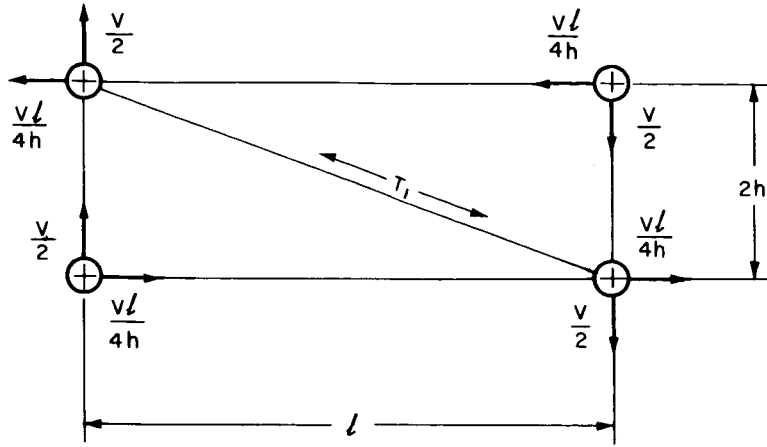


Figure 7—Shear Forces Acting at the Grid Points of a Diagonal Model Segment

where A is the area of that cross section. Timoshenko's shear coefficient k' is defined as

$$k' = \frac{Q}{\gamma G} , \quad (3.28)$$

where G is the shear modulus of the beam, and γ is the angle of shear at the neutral axis of the beam. Therefore equation (3.26) may be written as

$$T = \frac{\gamma k' AG}{4h} (4h^2 + \ell^2)^{1/2} . \quad (3.29)$$

The compliance of this diagonal tension element is by definition

$$C_d = \frac{\delta_1}{T} . \quad (3.30)$$

Using equations (3.24) and (3.29) and equating the angle of shear $\bar{\gamma}$ in the model to the angle of shear γ at the neutral axis of the beam, we have

$$C_d = \frac{8\ell h^2}{k' AG (4h^2 + \ell^2)} . \quad (3.31)$$

In summary, we have determined the distance of the grid points from the neutral plane (3.14), the compliance of the longitudinal tension elements (3.18), and the compliance of the diagonal tension elements (3.31), so that this diagonal model accounts for rotatory inertia, bending, and shear flexibility respectively, precisely those properties considered in the Timoshenko theory of the transverse vibrations of uniform beams.

EXAMPLES

1" × 1" × 25" Aluminum Cantilever Beam

As a first example, an aluminum cantilever beam was considered with the following parameter values.

1.0 in.	= Thickness
1.0 in.	= Depth
25 .0 in.	= Length
0.1 lb./in ³ .	= Weight density
1.0×10^7 lb/in ² .	= Young's modulus
4.0×10^6 lb/in ² .	= Shear modulus
.822	= Timoshenko's shear coefficient

This value of Timoshenko's shear coefficient, in addition to the method used to obtain it, can be found in reference (2).

The input data to the structural analysis computer program for the three finite element models with 25 partitions is shown in Table I.

Table II gives a comparison between the transverse frequencies of vibration of this beam as determined from the three beam theories and the three finite element models. The per cent error in the frequencies of the models was obtained by comparing the three digit bending model with the Bernoulli-Euler theory, the two digit bending model with the Rayleigh theory, and the diagonal model with the Timoshenko theory. The per cent error in frequency for most mode numbers, contrary to what one might suspect, was greatest for the three digit bending model. At the time of the writing of this paper, this fact was unexplained. It should be mentioned that when the two digit bending model was modified by excluding the moments of inertia at its grid points, the frequencies and mode shapes for this modified model agree exactly with the frequencies and

TABLE I
1" x 1" x 25" Aluminum Cantilever Beam
Finite Element Models with 25 Partitions

Input to the Structural Analysis Computer Program	Three Digit Bending Model	Two Digit Bending Model	Diagonal Model
Number of grid points	26	26	52
Distance of grid points from neutral plane (in.)			.289
Number of equations of equilibrium	27	51	104
Number of dynamic degrees of freedom	25	49	100
Mass at grid points excluding those at ends of model (lb. -sec ² /in.)	2.59 x 10 ⁻⁴	2.59 x 10 ⁻⁴	1.295 x 10 ⁻⁴
Moment of inertia at grid points excluding those at ends of model (lb. -sec. ² /in.)		2.16 x 10 ⁻⁵	
Number of structural elements	27	51	129
Complicace of three digit bending elements (lb./in. ²)	8.0 x 10 ⁻⁷		
Compliance of two digit bending elements (lb./in. ²)	4.0 x 10 ⁻⁷	4.0 x 10 ⁻⁷	
Coupled compliance of three digit bending elements (lb./in. ²)	2.0 x 10 ⁻⁷		
Coupled compliance of two digit bending elements (lb./in. ²)	2.0 x 10 ⁻⁷	2.0 x 10 ⁻⁷	
Compliance of longitudinal tension elements (lb./in. ²)			2.0 x 10 ⁻⁷
Compliance of diagonal tension elements (lb./in. ²)			1.52 x 10 ⁻⁷

TABLE II
1" x 1" x 25" Aluminum Cantilever Beam

Mode Number	Frequency in Radians Per Second						% Error in Frequency		
	Bernoulli-Euler Theory	Rayleigh Theory	Timoshenko Theory	Three Digit Bending Model	Two Digit Bending Model	Diagonal Model	Three Digit Bending	Two Digit Bending	Diagonal
1	319.1	319.0	318.7	318.8	318.7	318.5	.09	.09	.04
2	1999.5	1995.2	1982.3	1994.4	1990.4	1981.5	.26	.24	.04
3	5598.7	5570.1	5486.2	5575.4	5548.9	5490.7	.42	.38	.08
4	10971.3	10868.2	10575.5	10907.1	10812.8	10607.4	.59	.51	.30
5	18136.3	17866.6	17129.8	17999.6	17755.1	17230.5	.75	.62	.59
6	27092.4	26510.1	24990.1	26841.7	26318.4	25217.1	.93	.72	.91
7	37839.9	36735.3	33994.9	37422.4	36438.3	34412.5	1.10	.81	1.23
8	50378.5	48470.1	43988.2	49728.7	48043.3	44655.6	1.29	.88	1.52
9	64708.3	61636.0	54826.2	63744.7	61055.8	55783.1	1.49	.94	1.75
10	80829.5	76149.8	66380.0	79449.4	75393.3	67633.8	1.71	.99	1.89
11	98741.9	91924.8	78537.1	96811.8	90966.8	80048.7	1.95	1.04	1.93
12	118445.5	108873.4	91200.6	115789.1	107683.8	92873.0	2.24	1.09	1.83
13	139940.3	126907.3	104287.7	136322.4	125450.8	105956.0	2.59	1.15	1.60
14	163226.4	145940.0	117728.5	158306.5	144159.2	119147.5	3.01	1.22	1.21
15	188303.7	165886.9	131463.7	181604.4	163706.9	132293.0	3.55	1.31	.63
16	215172.2	186666.6	145443.6	206025.7	183990.6	145252.5	4.25	1.43	.13
17	243832.0	208201.5	159625.8	231302.8	204911.0	157870.1	5.14	1.58	1.10
18	274283.0	230418.3	173974.9	257021.9	226347.7	169974.1	6.29	1.77	2.30
19	306525.2	253247.9	188460.4	282595.5	248158.2	181382.6	7.81	2.01	3.76
20	340558.7	276626.4	203056.6	307426.4	270256.9	191926.3	9.73	2.30	5.48
21	376383.4	300494.2	217741.3	330752.3	292578.0	201402.8	12.12	2.63	7.50
22	413999.4	324796.7	232495.1	351550.6	314947.2	209593.6	15.08	3.03	9.85
23	453406.6	349483.6	247301.2	368933.3	337270.5	216296.6	18.63	3.49	12.54
24	494604.9	374509.3	262144.4	381995.8	359466.6	221263.3	22.76	4.02	15.59
25	537594.6	399832.0	277010.8	390151.6	381413.9	224331.5	27.42	4.61	19.02

TABLE III
1" × 1" × 25" Aluminum Cantilever Beam

Mode Number	Frequencies in Radians Per Second		
	Timoshenko Theory	Diagonal Model 50 Partitions	% Error
1	318.7	318.6	.011
2	1982.3	1982.1	.010
3	5486.2	5487.3	.020
4	10575.5	10583.2	.073
5	17129.8	17154.0	.141
6	24990.1	25043.8	.215
7	33994.9	34091.8	.285
8	43988.2	44139.5	.344
9	54826.2	55036.7	.384
10	66380.0	66645.7	.400
11	78537.1	78842.1	.388
12	91200.6	91513.9	.344
13	104287.7	104562.5	.263
14	117728.5	117903.7	.149
15	131463.7	131456.3	.006
16	145443.6	145153.0	.200
17	159625.8	158935.7	.432
18	173974.9	172744.5	.707
19	188460.4	186533.0	1.023
20	203056.6	200257.1	1.378
21	217741.3	213870.5	1.778
22	232495.1	227340.9	2.217
23	247301.2	240621.2	2.701
24	262144.4	253688.4	3.226
25	277010.8	266523.0	3.786

TABLE IV
1" x 1" x 25" Aluminum Cantilever Beam
Mode Shape Number 5

Distance Along Length of Beam in Inches	Displacements Normalized to 1 at the Tip					
	Bernoulli- Euler Theory	Rayleigh Theory	Timoshenko Theory	Three Digit Bending Model 25 Partitions	Two Digit Bending Model 25 Partitions	Diagonal Model 25 Partitions
0	0	0	0	0	0	0
1	.130	.130	.161	.133	.133	.155
2	.401	.402	.444	.410	.412	.441
3	.650	.654	.690	.667	.672	.696
4	.756	.763	.781	.778	.785	.798
5	.660	.669	.665	.683	.692	.690
6	.377	.386	.364	.396	.405	.390
7	-.013	-.005	-.038	-.002	.004	-.017
8	-.392	-.388	-.421	-.393	-.391	-.412
9	-.646	-.647	-.670	-.659	-.661	-.677
10	-.697	-.702	-.710	-.719	-.725	-.731
11	-.529	-.539	-.528	-.556	-.564	-.558
12	-.196	-.206	-.182	-.220	-.227	-.213
13	.198	.190	.221	.185	.180	.198
14	.532	.529	.556	.533	.532	.549
15	.700	.704	.721	.717	.721	.732
16	.652	.661	.664	.681	.688	.692
17	.403	.415	.404	.436	.445	.441
18	.032	.044	.024	.060	.069	.058
19	-.343	-.334	-.357	-.328	-.323	-.335
20	-.600	-.598	-.616	-.603	-.603	-.613
21	-.652	-.655	-.664	-.673	-.677	-.682
22	-.467	-.475	-.472	-.501	-.507	-.506
23	-.078	-.088	-.076	-.113	-.119	-.114
24	.438	.432	.445	.415	.411	.418
25	1.000	1.000	1.000	1.000	1.000	1.000

TABLE V
1" x 1" x 25" Aluminum Cantilever Beam
Mode Shape Number 10

Distance Along Length of Beam in Inches	Displacements Normalized to 1 at the Tip						
	Bernoulli Euler Theory	Rayleigh Theory	Timoshenko Theory	Three Digit Bending Model 25 Partitions	Two Digit Bending Model 25 Partitions	Diagonal Model 25 Partitions	Diagonal Model 50 Partitions
0	0	0	0	0	0	0	0
1	-.432	-.442	-.599	-.505	-.512	-.643	-.605
2	-.753	-.787	-.822	-.888	-.918	-.953	-.846
3	-.253	-.289	-.159	-.319	-.350	-.253	-.179
4	.526	.524	.650	.600	.598	.700	.657
5	.629	.662	.626	.757	.781	.763	.653
6	-.070	-.039	-.187	-.035	-.018	-.126	-.172
7	-.679	-.692	-.770	-.785	-.796	-.862	-.786
8	-.434	-.474	-.392	-.557	-.580	-.533	-.421
9	.360	.342	.475	.365	.361	.456	.468
10	.699	.727	.748	.832	.851	.880	.774
11	.154	.197	.086	.261	.278	.215	.115
12	-.585	-.581	-.683	-.635	-.643	-.716	-.687
13	-.585	-.627	-.599	-.739	-.760	-.761	-.633
14	.154	.117	.233	.078	.072	.136	.211
15	.699	.714	.775	.798	.814	.865	.791
16	.360	.411	.348	.523	.539	.523	.386
17	-.433	-.409	-.513	-.404	-.410	-.466	-.500
18	-.679	-.714	-.733	-.827	-.846	-.878	-.762
19	-.066	-.119	-.036	-.219	-.224	-.203	-.073
20	.631	.628	.709	.664	.679	.726	.710
21	.535	.589	.576	.723	.739	.764	.616
22	-.226	-.176	-.256	-.106	-.108	-.122	-.225
23	-.661	-.671	-.713	-.757	-.771	-.798	-.729
24	-.129	-.173	-.133	-.317	-.318	-.322	-.174
25	1.000	1.000	1.000	1.000	1.000	1.000	1.000

mode shapes obtained from the three digit bending model. Therefore, these large errors do not appear to be caused by some property peculiar to the three digit bending model.

It is interesting to note that for almost all mode numbers, the frequencies of the two digit bending model had the smallest error. However, the reader must bear in mind that the two digit bending model accounted for exactly those properties of a beam accounted for by the Rayleigh theory, which is less accurate in predicting the actual frequencies of a uniform beam than the Timoshenko theory. It is apparent from Table II that if the frequencies of all three models were compared with those of the Timoshenko theory, then the diagonal model would produce the smallest errors in frequency.

In order to decrease the per cent error in the frequencies of the diagonal model, the number of its partitions was increased from 25 to 50. The frequencies and per cent error in frequencies for this refined diagonal model are shown in Table III. We notice that the error in the first 16 frequencies was less than or equal to 0.4 per cent and that the error in the first 25 frequencies was less than 4.0 per cent.

In order to illustrate the degree of approximation of the mode shapes of these models to the mode shapes obtained from the three beam theories, two mode shapes, the fifth and tenth, are given in Tables IV and V respectively, and have been chosen to be representative of the results obtained for the other mode shapes. For these two mode shapes, the agreement between the models and the beam theories is fairly good.

10" × 5" × 25" Aluminum Cantilever Beam

In the previous example, the first 25 frequencies and mode shapes, according to the three beam theories, followed a very regular pattern. The frequencies were fairly evenly spaced and the n th mode shape always had n nodes, as should be expected. This regular pattern was due to the bending action in this beam being predominant in producing transverse vibration while shear flexibility, in the results according to the Timoshenko theory, produced only secondary effects. If thicker beams were considered, the results according to the Bernoulli-Euler and Rayleigh theories would again follow this regular pattern. However, it has been shown in reference (1) that for thick beams, in which shear flexibility is important, the frequencies no longer remain evenly spaced and it is possible for two mode shapes to have the same number of nodes. These results are a consequence of interactions between the bending and shear modes of vibration of the beam.

If the diagonal model is to be considered a good approximation to the Timoshenko beam, then the irregular pattern in the frequencies and mode shapes of thick beams, as predicted by the Timoshenko theory, must also occur in the frequencies and mode shapes of the diagonal model. For this reason the second example was chosen to be an aluminum cantilever beam 10 inches thick, 5 inches deep, and 25 inches long. The same parameter values for aluminum as used in the previous example, were used for this beam.

Table VI shows the frequencies obtained from the Timoshenko theory and the diagonal model with 50 partitions in addition to the per cent error in the frequencies of this model. We notice that the difference between the third and fourth frequencies is less than the difference between the second and third frequencies for both the theory and the model. In other words, the rate of change between consecutive frequencies is decreasing, a fact which was not true for the frequencies, according to the Timoshenko theory, of the previous example. The reason for this is due to a strong coupling between the bending and shear modes of vibration which occurs just beyond the fourth mode number. This phenomenon is discussed in both references (1), and (2). In addition, we notice that the errors in the first 25 frequencies of the model, with the exception of the 22 nd, are all less than 2.0 per cent, and the pattern in these errors is much more erratic than in the previous example.

Table VII shows the fourth, fifth, and eleventh mode shapes for both theory and model. We notice that both the fourth and fifth mode shapes have only four nodes and that the fifth mode shape has an unusual configuration at the free end. This phenomenon has also been noted in reference (1). In addition, we notice that the agreement between the Timoshenko theory and the diagonal model for these two mode shapes is excellent. This appears to be in sharp contrast to the results for the eleventh mode shape, in which the patterns are the same, but the magnitude of most displacements is about five and one half times greater for the Timoshenko theory than for the diagonal model. However, this disagreement is only apparent, for if each mode shape had its largest component of displacement normalized to one, then the displacements at the other points along the length of the beam and model would agree more favorably. The comparison between the other mode shapes according to the Timoshenko theory and the mode shapes of this diagonal model showed similar agreement. Therefore, the diagonal model does give good approximations to the transverse frequencies and mode shapes of a cantilever beam as obtained from the Timoshenko theory, even for very thick beams.

TABLE VI
Frequencies of a 10" × 5" × 25" Aluminum Cantilever Beam

Mode Number	Frequency in Radians Per Second		
	Timoshenko Theory	Diagonal Model 50 Partitions	% Error
1	2861.9	2861.6	.027
2	12097.7	12095.1	.021
3	25910.2	25895.0	.058
4	37716.1	37689.8	.070
5	47094.1	47058.5	.075
6	52495.8	52423.9	.137
7	62311.0	62192.8	.190
8	70175.9	69973.1	.289
9	78956.2	78724.5	.293
10	87179.9	86728.3	.518
11	98134.6	97742.3	.400
12	102856.5	102091.8	.744
13	117245.7	116070.5	1.002
14	120262.8	119600.8	.551
15	132359.6	130627.8	1.308
16	141958.4	140607.6	.952
17	147824.0	145807.4	1.364
18	159883.9	156891.9	1.871
19	167721.0	166172.4	.923
20	174826.2	173080.3	.999
21	189110.3	189324.5	.113
22	191125.4	198161.7	3.682
23	203759.9	205859.9	1.031
24	214180.1	213119.3	.495
25	218725.6	221291.4	1.173

TABLE VII
10" x 5" x 25" Aluminum Cantilever Beam

Distance Along Length of Beam in Inches	Displacements Normalized to 1 at the Tip					
	Mode Shape 4		Mode Shape 5		Mode Shape 11	
	Timoshenko Theory	Diagonal Model 50 Partitions	Timoshenko Theory	Diagonal Model 50 Partitions	Timoshenko Theory	Diagonal Model 50 Partitions
0	0	0	0	0	0	0
1	-.897	-.897	-.402	-.403	-39.513	-7.339
2	-1.649	-1.648	-.763	-.765	-61.309	-11.313
3	-2.142	-2.140	-1.007	-1.009	-45.704	-8.316
4	-2.302	-2.301	-1.081	-1.083	.382	.257
5	-2.105	-2.105	-.968	-.970	47.723	8.907
6	-1.579	-1.580	-.691	-.693	65.846	12.024
7	-.803	-.805	-.308	-.308	45.083	7.975
8	.110	.107	.104	.105	3.120	.207
9	1.024	1.020	.458	.460	-28.789	-5.451
10	1.804	1.800	.648	.686	-29.412	-5.216
11	2.334	2.330	.737	.738	-3.062	-.134
12	2.537	2.533	.610	.610	24.594	4.884
13	2.383	2.380	.336	.334	27.095	5.009
14	1.897	1.894	-.022	-.025	-1.691	-.632
15	1.151	1.149	-.382	-.385	-42.101	-8.139
16	.258	.257	-.661	-.664	-63.165	-11.736
17	-.648	-.647	-.794	-.797	-46.158	-8.188
18	-1.431	-1.429	-.748	-.749	.680	.638
19	-1.973	-1.970	-.527	-.526	47.486	9.036
20	-2.192	-2.189	-.173	-.170	64.329	11.614
21	-2.053	-2.051	.243	.248	42.829	7.215
22	-1.577	-1.575	.636	.642	1.664	-.361
23	-.833	-.831	.927	.932	-28.050	-5.337
24	.070	.071	1.057	1.059	-26.334	-4.366
25	1.000	1.000	1.000	1.000	1.000	1.000

4. CONCLUSIONS

Three different finite element models of a $1'' \times 1'' \times 25''$ aluminum cantilever beam have been used to approximate its frequencies and mode shapes. Most significant among these models was the diagonal model in which bending, rotatory inertia, and shear flexibility were considered. The first seventeen frequencies of the diagonal model with twenty five partitions differed from those according to the Timoshenko theory by less than 2 per cent. If shear flexibility is not to be considered, then the number of degrees of freedom can be halved by using a two digit bending model while maintaining the same number of partitions. We have seen that the first eighteen frequencies of the two digit bending model with twenty five partitions differed from those according to the Rayleigh theory by less than 2 per cent. If only bending is to be considered, then the number of degrees of freedom can be halved again by using a three digit bending model for the same number of partitions. The first eleven frequencies of this model with twenty five partitions differed from those according to the Bernoulli-Euler theory by less than 2 per cent.

The real value of the diagonal model as an analytical tool was realized when an aluminum cantilever beam 10'' thick, 5'' deep, and 25'' long was considered. According to the Timoshenko theory, it is possible for two mode shapes to have the same number of nodes. This phenomenon was exhibited in the first twenty five mode shapes of the diagonal model with fifty partitions in exactly the same way as in the mode shapes according to the Timoshenko theory. In addition, the first twenty five frequencies, with the exception of the twenty second, of this diagonal model differed from those according to the Timoshenko theory by less than 2 per cent. Therefore, the diagonal model does provide a good approximation to the transverse frequencies and mode shapes of uniform cantilever beams.

REFERENCES

1. Traill-Nash, R.W., and Collar, A.R.: The Effects of Shear Flexibility and Rotatory Inertia on the Bending Vibrations of Beams. *Quarterly Journal of Mechanics and Applied Mathematics*, Vol. VI, Part 2, 1953, pp. 186-222.
2. Mindlin, R.D., and Deresiewicz, H.: Timoshenko's Shear Coefficient For Flexural Vibrations of Beams. *Proceedings of the 2nd U.S. National Congress of Applied Mechanics*, 1954, pp. 175-178.